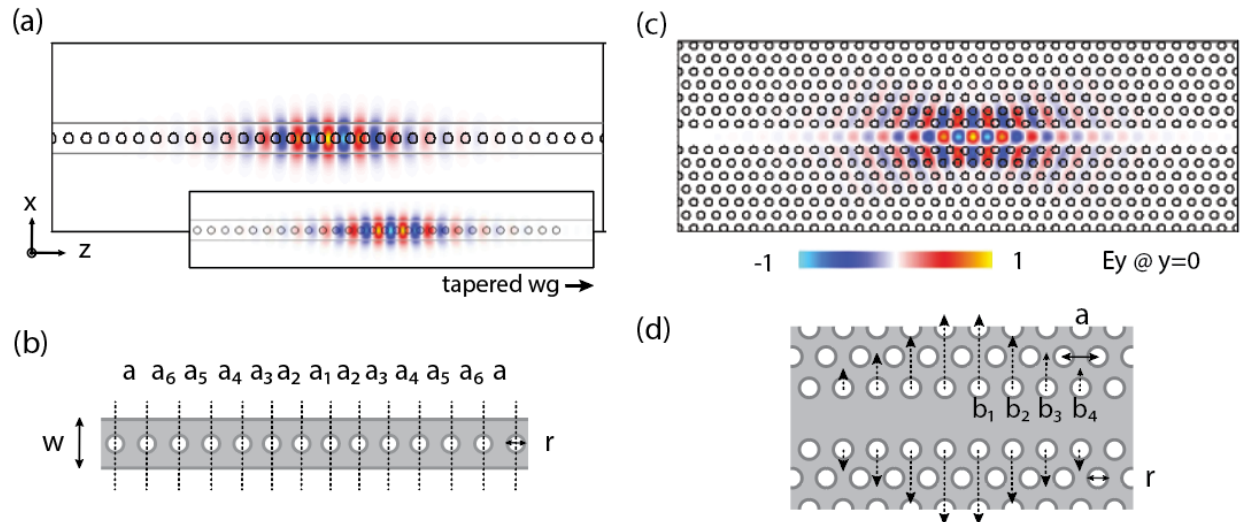


## Supplementary Information

### Device design

The 1D and 2D PhCs in this paper are simulated using a 3D finite-difference time-domain (FDTD) method. They share the same geometry as in a previous work<sup>1</sup>. Fig. S1 (a) and (b) show the mode profile and the geometry of the cavity region of the 1D PhC cavity. Fig. S1 (a) inset shows the mode profile of the 1D PhC device coupled to a feeding waveguide. The free-standing diamond nanobeam is designed to be 370 nm wide ( $w$ ), and 160 nm thick ( $d$ ). For the mirror cells, we scan the lattice constant  $a$  from 226 nm to 284 nm, to cover a wide range of target wavelength from 680 nm to 800 nm of the cavity. The airhole radius ( $r$ ) is 65 nm. To form the cavity, we taper the lattice constant at the center quadratically, with  $a_1 = 0.84a$ ,  $a_2 = 0.844a$ ,  $a_3 = 0.858a$ ,  $a_4 = 0.88a$ ,  $a_5 = 0.911a$ ,  $a_6 = 0.951a$ . Fig. 1 (b) shows the electric field profile ( $E_y$ ) of the fundamental mode of the cavity with  $a = 269$  nm. The simulated  $Q$  is  $1.3 \times 10^6$ , with a mode volume of  $V \sim 0.5(\lambda/n)^3$ . The waveguide-coupled devices are designed by removing 9 holes from one side of the 1D PhC device. The holes that form the cavities have the same dimensions. When  $a$  is set to be 255 nm for the devices with tapered waveguides, the simulated  $Q$  is  $1.9 \times 10^5$ , with a mode volume of  $V \sim 0.5(\lambda/n)^3$ . The coupling efficiency between the cavity and diamond waveguide  $\eta_c$  is simulated to be  $\sim 87\%$  by FDTD simulations.

Fig. S1 (c) and (d) show the mode profile and the geometry of the cavity region of the 2D photonic crystal. The cavity is created by the local width modulation of a line defect. The lattice is triangular, where the lattice constant ( $a$ ) ranges from 236 nm to 269 nm to target wavelength from 677 to 767 nm, and the hole radius ( $r$ ) is also 65 nm. By keeping the air hole size constant across a given chip, we can minimize systematic distortion in the hole sizes in fabrication. The cavity is formed by removing a row and shifting the central holes “outwards” towards the mirror region in a linear fashion, where  $b_1 = 10.1$  nm,  $b_2 = 0.75b_1$ ,  $b_3 = 0.5b_1$ ,  $b_4 = 0.25b_1$ . Fig. 1 (d) shows the electric field profile ( $E_y$ ) of the fundamental mode of the cavity with  $a = 252$  nm. The simulated  $Q$  is  $6.3 \times 10^6$ , with a mode volume of  $V = 2.9(\lambda/n)^3$ .



**Fig. S1** (a) 1D phC mode profile ( $E_y$ ). The field is normalized. (b) 1D phC design. The cavity is formed by tapering the lattice constant quadratically,  $a_1$  to  $a_6$ . (c) 2D phC mode profile ( $E_y$ ). (d) 2D phC design. The cavity is formed by shifting the holes, by  $b_1$  through  $b_4$ .

### Fiber-coupling measurements

We can estimate the degree of over/under coupling via the depth of the cavity reflection dip  $R_0$  via the formula  $\kappa_i = \frac{\kappa(1 \pm \sqrt{R_0})}{2}$  where the plus (minus) refers to the cavity being over (under) coupled. For the cavities, where  $R_0$  is close 0, this is a signature of the cavities being near-critically-coupled ( $\kappa_e \sim \kappa_i$ ). For the fitted 95.4% contrast, the  $Q_i$  and  $Q_e$  are estimated to be  $1.4 \times 10^5$  and  $2.2 \times 10^5$ , interchangeably.

In order to calculate coupling efficiency, it is necessary to decouple setup-related losses from losses related to the fiber-device coupling interface. We can express this mathematically by writing the total loss from D1 to D2 ( $\eta_{tot}$ ) as a product of these losses, i.e.  $\eta_{tot} = \eta_s \eta_c^2$ . To find  $\eta_s$ , we splice a retroreflector into the setup at port 2, such that the loss from D1 to D2 can be solely attributed to setup losses  $\eta_s$ . Once this is calibrated, we can attribute any excess losses in the device measurement as fiber-device coupling losses.

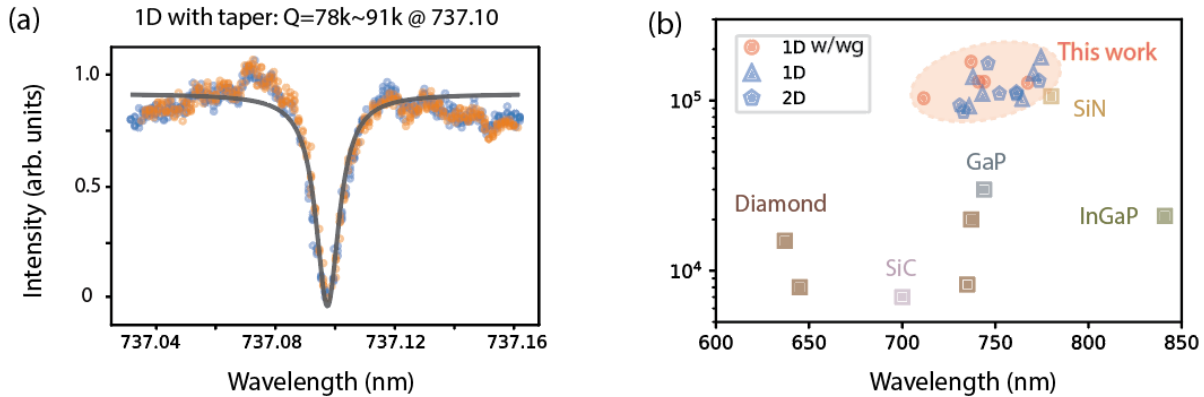


**Fig. S2 Q measurement summary.** (a) The forward and backward scan of the waveguide-coupled 1D PhC shown in the main text. (b) A summary of the Qs obtained from on-resonance laser scans for all devices on the sample, compared with the highest literature Q factors in diamond 1D and 2D PhC.

To confirm that the peaks are not broadened or narrowed because of thermo-optics caused by the laser sent into the cavity, we scanned both forward and backward with the same scanning speed and laser power. The fitted Q is between  $7.8 \sim 9.1 \times 10^4$ , as shown in Fig. S2 (a).

We can resolve the devices with resonances reachable by the scanning laser, in the range of 710-790 nm. They are plotted in Fig. S2 (b) against literature values presented in Table 1, which is an extended version of Fig. 4. (g) in the main text.

### Calculating Purcell Factor and Cooperativity

The Purcell factor of the investigated zero-phonon line (ZPL)  $F_{ZPL}$ , is estimated using the following equation<sup>2</sup>:  $F_{ZPL} = (\tau_{off}/\tau_{on} - 1)/\varepsilon_{ZPL}$ , where  $\varepsilon_{ZPL}$  is defined by the fraction of the total emission into the ZPL visible at 4K for an SiV, which is estimated by a product of the Debye–Waller factor of 70%<sup>3</sup> and the branching ratio of 19.3% into D line at 4K<sup>2</sup>. We use an exponential with a constant offset to fit the lifetimes in the main text ( $\tau_{on}$  and  $\tau_{off}$ ). The constants are fitted to be  $51 \pm 2$  and  $38 \pm 2$ , which are contributed to the dark counts of the system. For this estimation, we also assume that the lifetime of a SiV measured in unpatterned area  $\tau_{bulk}$  ( $\sim 1.2$  ns) is equal to the off-resonance value<sup>2</sup>. Notice, the extracted Purcell factor of 13 is consistent with the  $\sim 20$ -fold relative increase in photon rate at the D line when the cavity is tuned into resonance with it. The error could come from the limited resolution of the spectrometer (1800 gr/mm).

The theoretical Purcell factor is obtained from the following equation:  $F \equiv \frac{3}{4\pi^2} \frac{\lambda^3}{n^3} \frac{Q}{V}$ . The theoretical value is dictated entirely by the cavity parameters. We use the measured  $Q \sim 1.2 \times 10^5$  and simulated  $V \sim 0.5(\lambda/n)^3$ , and estimated  $F$  to be  $1.8 \times 10^4$  in the most ideal case.

The cooperativity is calculated using  $C = 4g^2/(\kappa\gamma)$ , where  $g$  is the coupling rate between the SiV and the cavity,  $\kappa$  and  $\gamma$  are the decay rate of the cavity and the emitter, respectively. If the SiV is placed at the cavity field maximum, the estimated  $g$  is 15.2 GHz, and experimentally, it has been observed to be  $\sim 8$  GHz<sup>4</sup>. The SiV linewidth is  $\gamma \sim 0.12$  GHz at  $\sim 100$  mK<sup>4</sup> or  $\gamma \sim 0.61$  GHz as measured in this work at  $\sim 4$ K, and the measured highest  $Q$  is  $1.8 \times 10^5$  ( $\kappa \sim 2.2$  GHz) or  $8.4 \times 10^4$  ( $\kappa \sim 4.8$  GHz) in the critically-coupled case. Using the ideal numbers, a  $C$  as large as 3500 at 100 mK can be obtained. Using the observed  $g \sim 8$  GHz, the obtained values are  $C \sim 970$  or  $C \sim 440$  at 100 mK. Using the observed  $g$  and linewidth of SiV at 4K from this work, the obtained values are  $C \sim 190$  or  $C \sim 87$  at 4K.

## References

1. K. Kuruma. *et al.* Coupling of a Single Tin-vacancy Center to a Photonic Crystal Cavity in Diamond. *Appl. Phys. Lett.* 118, (2021).
2. Zhang, J. L. *et al.* Strongly Cavity-Enhanced Spontaneous Emission from Silicon-Vacancy Centers in Diamond. *Nano Lett.* **18**, 1360–1365 (2018).
3. Aharonovich, I. *et al.* Diamond-based single-photon emitters. *Rep. Prog. Phys.* **74**, 076501 (2011).
4. Bhaskar, M. K. *et al.* Experimental demonstration of memory-enhanced quantum communication. *Nature* **580**, 60–64 (2020).